

# High Frequency Transformer Design Report

## Work Package 4

OZAN KEYSAN  
*University of Edinburgh*  
September 17, 2014

### Abstract

This report presents the material options for the core of the medium frequency transformer that is being investigated within the Work Package 4 of the “Next Generation HVDC Network for the Energy Industry” project.

*Keywords:* medium frequency transformer, HVDC transmission, core losses, HV transformer

## 1 Introduction

A literature review is presented by Robert Fox within WP 2, in which different medium-frequency transformers were compared and the components of medium-frequency transformers are listed. This report will focus on the suitable core materials for medium frequency transformers and the main loss components.

Transformers are the bulkiest part of the medium voltage conversion systems [1, 2]. Thus, there is a trend to reduce the size and weight of these components. In [3], it is stated that the weight and size of a 3 MW 1.2 kHz transformer is less than 8% of an equivalent 50 Hz line transformer. In Fig. 1, volume variation with operating frequency for a 1 MW transformer is presented. However, as the frequency is increased, skin effect, proximity effect, hysteresis losses and dielectric losses are significantly increased. Furthermore, the reduction in size usually implies same power loss in much smaller area, which demands forced cooling techniques as in [4].

In the transformer design, types of challenges change with increasing frequency. Important design factors in conventional line transformers and

Line Transformer (50 Hz)	High Frequency Transformer
Core Mass	Skin Effect
Copper Losses	Core Losses
Volume	Parasitic Capacitance
	Cooling
	Resonance

Table 1: Important factors in the design of line frequency and high-frequency transformers.

high frequency transformers are tabulated in Table 1. However, challenges of medium to high frequency transformers can be listed as [5]:

- Loss reduction for higher frequency range.
- Efficient thermal management, higher power levels are contained in equal volumes.
- High-dielectric stress generated by rapidly changing rectangular voltage waveforms.
- High-isolation levels are required (due to multi-level inverter structure).
- Generation of acoustic noise, which reaches the most sensitive range of the human ear.

## 2 Core Materials

Although, silicon or nickel-steel laminations are commonly used in conventional line frequency power transformers, the high loss of these components at high frequencies makes other options more viable. Ferrite is one of the first alternatives in the market, but in the recent years materials like amorphous and nanocrystalline become increasingly popular [1].

### Amorphous Materials

Amorphous cores are typically made of Metglas (metallic glass alloy), which is a thin non-crystalline amorphous metal alloy of iron, boron, silicon and phosphorus. The material has a much higher resistivity in electrical steel which results in a low eddy losses. Furthermore, the hysteresis losses of amorphous cores are lower, which reduces the no-load losses compared to

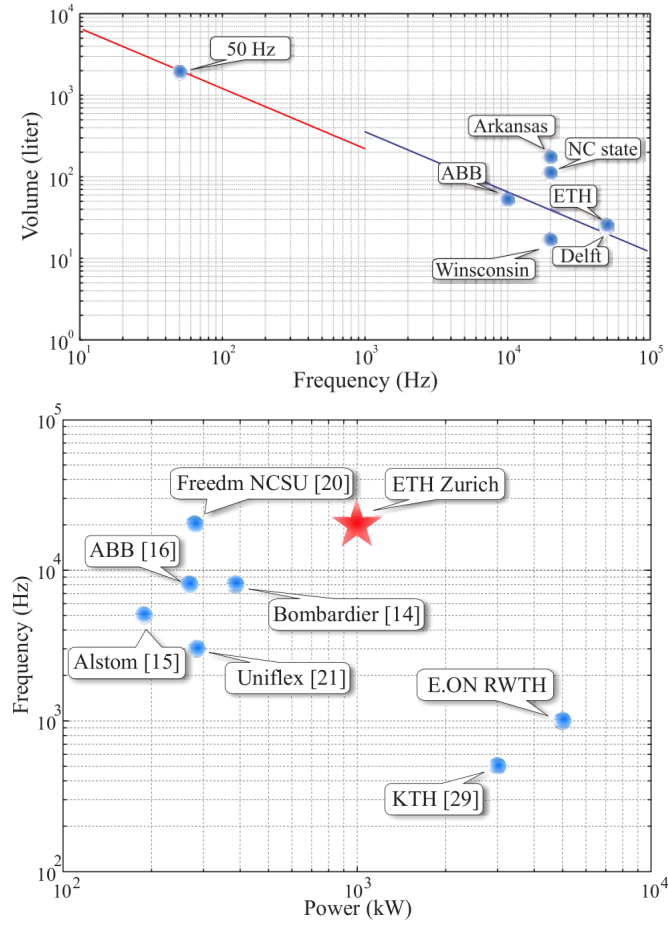


Figure 1: Volumes of high frequency transformers(normalized to 1 MW) and rated power and operating frequencies of existing DC-DC converter prototypes [6, 7].

	Amorphous (Vitrovac)	Nano-crystalline (VitroPerm)
Saturation Flux Density	0.8 T	1.2 T
Losses (f= 20 kHz, B=0.2 T)	2 W/kg	1.4 W/kg
Max. Operating temperature	110 °C	120 °C
Curie temperature	365 °C	600 °C

Table 2: Comparison of amorphous (Vitrovac) and nano-crystalline (VitroPerm) materials [8].

one with electrical steel. However, amorphous materials usually have lower saturation flux density compared to conventional iron-silicon electrical steel.

Some manufacturers of amorphous transformer cores can be listed as:

- Hitachi Metals (Powerlite)
- Vacuumschmelze (Vitrovac)
- Metglas
- Vijai Electricals

Although, amorphous materials are superior to electrical steel laminations, nano-crystalline materials are superior to amorphous materials with their lower cost and higher flux densities [8]. Nano-crystalline materials will be discussed in the next section. The specifications of amorphous and nano-crystalline materials are compared in Table 2. The only application that a amorphous material can be more advantageous is high-frequency single-ended forward converter topologies. For all other topologies, nano-crystalline materials are considered to be more suitable.

### Nano-crystalline

Nano-crystalline is a fairly new material that consists of approximately 80% of iron with the remaining is mixture of silicon, boron, carbon, nickel and other materials. This is a special type of amorphous material, which has superior magnetic characteristics, such as lower core loss and high permeability. Other specifications can be listed as [9]:

- Up to 50 % permeability than 80% nickel material (e.g. Supermalloy).
- High saturation flux density (1.2-1.5 T).
- High operating temperature up to 130 °C.
- Minimal change of magnetic characteristics with temperature.

- 17 % lighter than Nickel with a density of  $7.3 \text{ g/cm}^3$ .
- Stacking density up to 90 % can be achieved.

Some main manufacturers of nano-crystalline materials can be listed as:

- MK Magnetics
- Vacuumschmelze
- Hill-Tech

In this section, different types of nano-crystalline materials will be compared. Vacuumschmelze manufactures various soft magnetic nano-crystalline materials under the brand of VitroPerm.

### **VitroPerm**

Nanocrystalline VitroPerm alloys are based on Fe with Si and B with Nb and Cu additives [10]. VitroPerm nano-crystalline alloys are optimized to combine highest permeability and lowest coercive field strength. The combination of very thin tapes and the relatively high electrical resistance ( $1.1\text{-}1.2 \mu\Omega\text{m}$ ) to ensure minimal eddy current losses and an outstanding frequency vs. permeability behaviour. Along with saturation flux density of 1.2 T and wide operational temperature range, these features combine to make VitroPerm superior in many aspects to commonly used ferrite and amorphous materials. Magnetization curves and B-H characteristics of VitroPerm materials are presented in Fig. 2.

VitroPerm has a wide range material options with different permeability scale as shown in Fig. 3. The permeability of VitroPerm 500F is significantly higher than ferrite as shown in Fig. 4.

VitroPerm has also a high operating temperature compared to ferrite. The Curie temperature of VitroPerm alloys are  $600^\circ\text{C}$ . Furthermore, the saturation flux density only reduces by 10% at  $120^\circ\text{C}$ , which allows the core can be overloaded for short-amount of periods up to  $180 - 200^\circ\text{C}$ . The variation of permeability with temperature for VitroPerm is presented in Fig. 5.

### **Silicon-Steel**

Silicon-steel is a popular choice in line frequency power transformers for its low cost and high-saturation magnetic induction. However, core losses of silicon-steel is high compared to other materials, which makes them unsuitable for medium frequency transformers. The core losses of material will be compared in the next section.

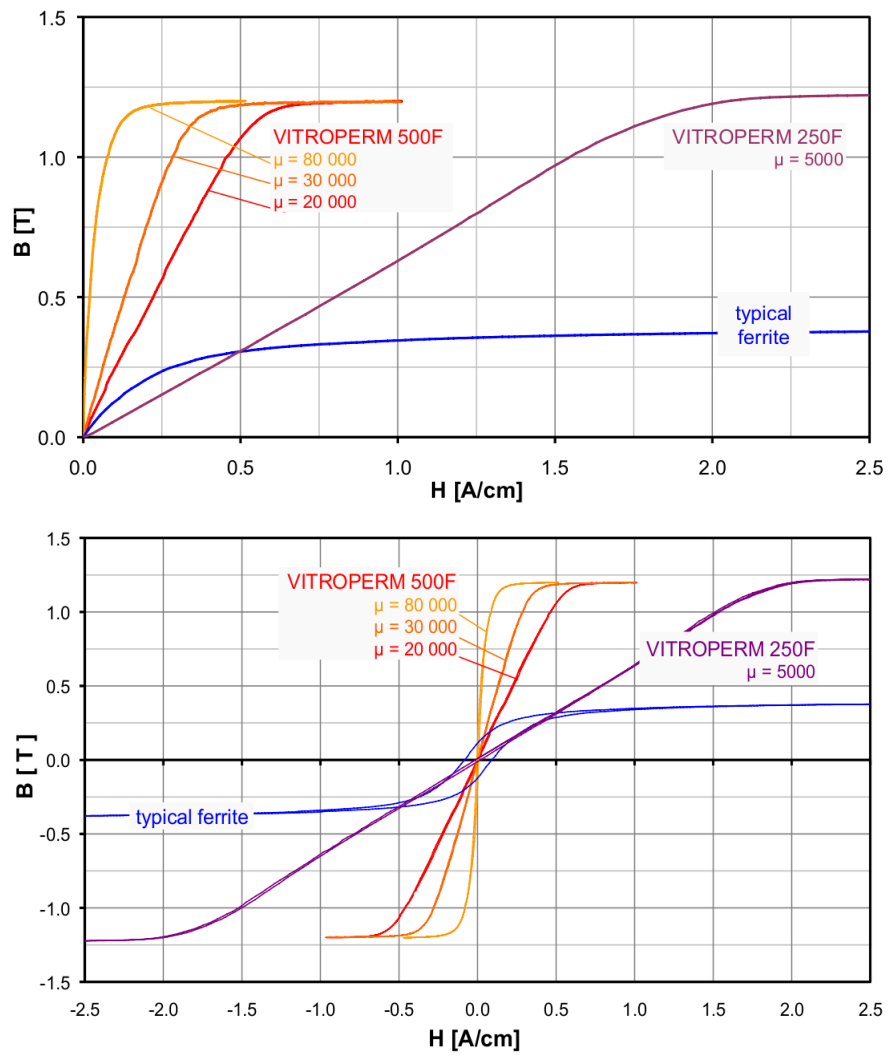


Figure 2: Magnetisation curve and B-H characteristics of VitroPerm [10].

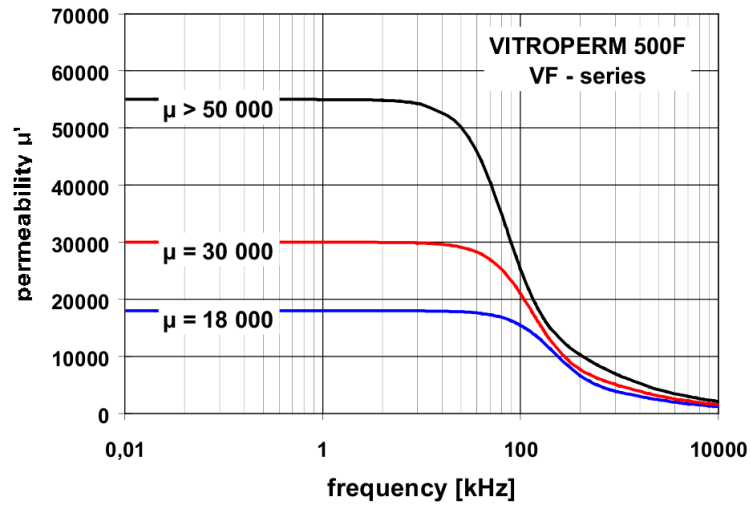


Figure 3: Permeability change of different VitroPerm materials with frequency [11].

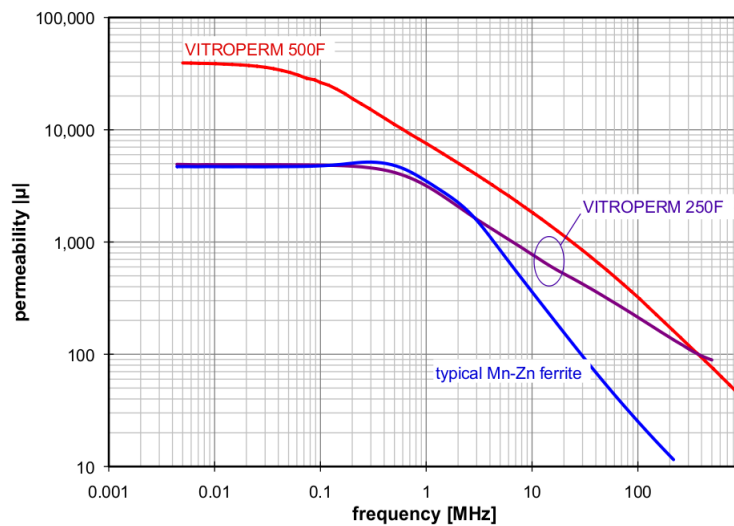


Figure 4: Permeability change of VitroPerm 250F( $\mu = 5000$ ), VitroPerm 500F( $\mu = 40000$ ) and ferrite( $\mu = 5000$ ) with frequency. [10].

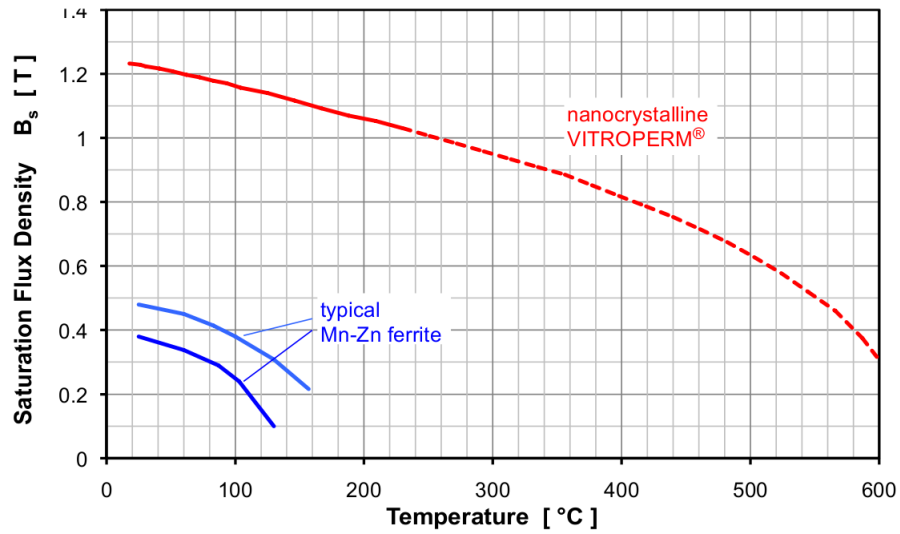


Figure 5: Saturation flux density variation of VitroPerm with temperature.

## Ferrites

Ferrites have a low-loss density in very high-frequencies, which makes them a suitable material for high-frequency applications such as RF-filters and chokes. However, they have saturation flux density around 0.5 T, which increases the core volume and mass in high power applications.

## Core Material Comparison

Different core materials and manufacturers are presented in Table 3. In Fig. 6, prototypes with common core materials are presented. It can be seen from the table that nano-crystalline and amorphous materials are the most suggested materials for medium frequency transformers that work between 1 kHz and 25 kHz.

The hysteresis losses and the core loss of different materials are compared in Fig. 7. Core losses are presented in Fig. 8. It can be seen that between 1 kHz and 10 kHz, the core loss of 0.3 mm silicon-steel laminations are 25 times higher than nano-crystalline material. A 50 kV, high frequency (20 kHz), 150 kW transformer that uses nano-crystalline material is presented in [14], in which the core losses are estimated as 60W/kg at an operating flux density of 1 T.



Frequency	Magnetic Material	Low-Leakage Inductance Resonant Converter	High-Leakage Inductance Non-Resonant Converter
< 1 kHz	Silicon-Steel (FeSi)		<b>Traction, 75 kVA</b> 400 Hz, Bare 340 $\mu$ H, Oil [Hugo et al., 2007]
1 kHz to 25 kHz	Nanocrystalline	<b>Traction, 350 kVA</b> 10 kHz, Coaxial < 50 kg, 3 $\mu$ H, Water [Heinemann, 2002]	<b>General, 10 kVA</b> 20 kHz, Litz wire 1.6 $\mu$ H + $L_{ext}$ 21 $\mu$ H [Akagi and Inoue, 2006]
		<b>Traction, 500 kW</b> 8 kHz, Coaxial 2.3 $\mu$ H, Water, 18 kg [Steiner and Reinold, 2007]	<b>Traction, 1 MVA</b> 4 kHz, Litz wire 215 $\mu$ H, 148 kg, Cyclo [Kjellqvist et al., 2004]
	Amorphous	<b>General, 50 kW</b> 25 kHz, Interleaved Foils 3 $\mu$ H + $L_{ext}$ 37 $\mu$ H [Pavlovsky et al., 2005]	<b>Wind, 280 kVA</b> 1.2 kHz, Coaxial 251 nH, Passive Rectifier [Prasai et al., 2008]
			<b>Wind, 1 MW</b> 10 kHz, HV Litz wire 50 $\mu$ H, Passive Rectifier [Morren et al., 2001]
> 25 kHz	Ferrite		<b>Wind, 3.6 kW</b> 50 kHz, Litz wire 14 $\mu$ H, Passive Rectifier [Morren et al., 2001]
			<b>General, 50 kW</b> 50 kHz, Coaxial 1.6 $\mu$ H [Kheraluwala et al., 1992]
			<b>Drives, 25 kW</b> 50 kHz, Litz wire 2.2 mH, Forced Air [Aggeler et al., 2008]

Figure 6: Common materials used in medium frequency transformers and previous prototypes (Heinemann, 2002:[4], Steiner,2007:[2], Pavlovsky,2005:[12], Morren,2002:[13], Prasai,2007:[3]) [5].

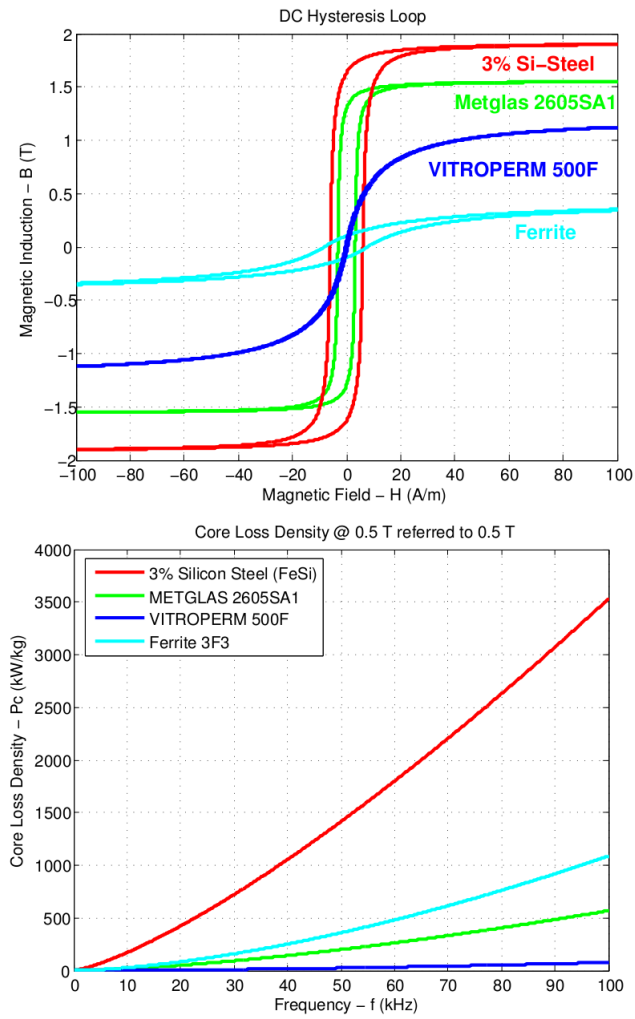


Figure 7: Loss comparison of silicon-steel, amorphous, nano-crystalline and ferrite materials [5]. a) Hysteresis loss, b) Core loss.

Material	Brand	Saturation Flux	Core Loss	Manufacturer
Amorphous	Microlite	1.56 T	1.5 kW/kg	Metglas
	Powerlite	1.56 T	0.6 kW/kg	Metglas
	Namglass	1.59 T	0.34 kW/kg	Magmet
	Vitrovac	0.82 T	0.19 kW/kg	VAC
Nano-crystalline	Finemet	1.23 T	0.14 kW/kg	Hitachi
	VitroPerm	1.2 T	0.07 kW/kg	VAC
	Nanoperm	1.2 T	0.04 kW/kg	Magnetec
	Namglass 4	1.23 T	0.04 kW/kg	Magmet
Silicon Steel	Arnon 7	1.53 T	1.6 kW/kg	Arnold
	Arnon 5	1.48 T	1.06 kW/kg	Arnold

Table 3: Core materials and manufacturers for high-frequency transformers (specific losses at  $B = 1$  T,  $f = 20$  kHz) [7].

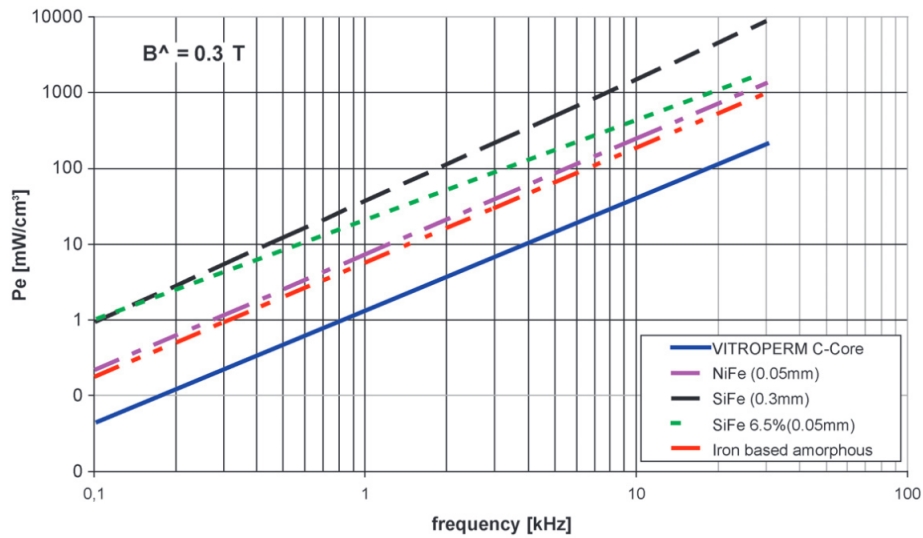


Figure 8: Core loss comparison of nano-crystalline (VitroPerm) with electrical steel and amorphous material [10].

### 3 Losses in a Transformer

There are many analytical models to calculate the losses of medium frequency transformers. These methods, for different transformers types are reviewed in [1] and in [5].

#### 3.1 AC Winding Losses

The high frequency excitation in a medium frequency transformer has two main effects in the transformer windings:

- Skin Effect: In AC excitation the current itself generates an opposing magnetic field and current, which reduce the net current density inside the conductor. The total current will stay same, but the distribution will be higher across the circumference of the conductor.
- Proximity Effect is the interaction between two adjacent conductors that alters the current distribution in the conductor. Same principles(e.g. proximity, frequency) apply in the proximity affect.

Losses due to skin effect decrease by increasing the foil thickness whereas proximity effect losses increase with increasing foil thickness [7].

##### 3.1.1 Skin Effect

Skin effect is an important factor in AC resistance and eddy current losses in a transformer. Skin effect is effected by the skin depth, which can be expressed as:

$$\sigma = \sqrt{\frac{2\rho}{\mu\omega}} \quad (1)$$

where  $\rho$  is the resistivity of the conductor,  $\mu$  is permeability, and  $\omega$  is the frequency in rad/s. Skin depth of copper for different operating frequencies are presented in Table 4. For reasonable AC resistance characteristics, the rule of thumb is to choose the conductor diameter smaller than 1.6 times of the skin depth. Thus, for a 1-2 kHz transformer application, the conductor should not be thicker than 2-3 mm.

In a step-up transformer the cross-section area of the primary conductor will be larger. However, the limit due to skin-depth limits the thickness of the conductor. Therefore, the most feasible way is to use foil conductors in the primary windings. Dowell calculated eddy losses in foil type transformer windings in [15]. A detailed explanation of these one dimensional Maxwell equations can be found in [5] and a summary will be presented in this section.

Frequency	Skin Depth
50 Hz	9.2 mm
1 kHz	2.06 mm
2 kHz	1.49 mm
5 kHz	0.94 mm
10 kHz	0.65 mm
50 kHz	0.29 mm

Table 4: Skin depth in a copper conductor.

The DC resistance of a foil winding can be expressed as:

$$R_{dc} = \rho \frac{L_{mean}}{t_w h_w} N_{turns} \quad (2)$$

where  $L_{mean}$  is the mean turn length of the coil,  $t_w$  is the thickness,  $h_w$  is the height,  $\rho$  is the resistivity of copper.

The AC resistance is more complicated to calculate and depends on the ratio of the wire thickness to skin depth ( $\delta$ ) and can be expressed as:

$$R_{ac} = \rho \frac{L_{mean}}{h_w \delta} N_{turns} \left[ \zeta_1 + \frac{2}{3} (N_{turns}^2 - 1) \zeta_2 \right] \quad (3)$$

where:

$$\zeta_1 = \frac{\sinh(2\Delta) + \sin(2\Delta)}{\cosh(2\Delta) - \cos(2\Delta)} \quad \zeta_2 = \frac{\sinh(\Delta) - \sin(\Delta)}{\cosh(\Delta) + \cos(\Delta)} \quad \Delta = \frac{t_w}{\delta} \quad (4)$$

as can be seen from the equation above, the important factor is the penetration factor (i.e the ratio of conductor thickness to skin depth,  $\Delta$ ). The ratio of AC resistance to DC resistance is called Dowell's resistance factor ( $F_r$ ). The resistance factor as a function of penetration ratio for a 2 mm thick foil wire is presented in Fig. 9. For example, at 1 kHz the skin depth is 2.1 mm (the penetration ratio is approximately 1), the resistance factor is 2.7 for a layer number of 4. Thus the resistive losses will be 2.7 times more compared to DC conduction.

### 3.1.2 Secondary-Winding

There are different analytical models to estimate the AC resistances of round conductors (e.g. high voltage cables that can be used in the secondary winding), such as presented in [16, 17]. Although, the method presented by Dowell in [15] is assumed as the most established method. In this method

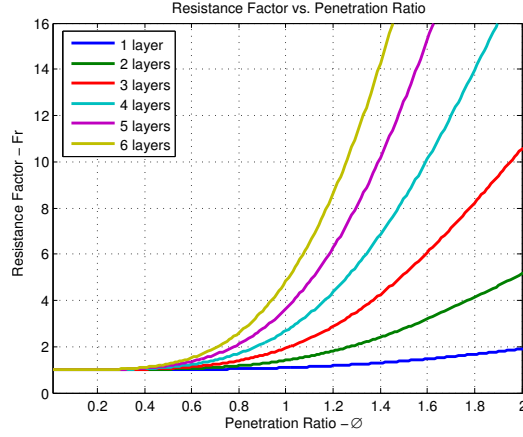


Figure 9: Resistance factor for a function of penetration ratio (for 2 mm thick foil conductor) [5].

Dowell introduced a porosity factor to convert the round conductors to square conductors and then convert to foil type conductors.

Equivalent thickness of a round conductor can be defined as [15]:

$$d_w = \sqrt{\frac{\pi}{4}}d \quad (5)$$

where  $d$  is the diameter of the round conductor and  $d_w$  is the thickness of the equivalent square conductor. Then, similar technique can be applied to convert square conductor to foil type conductor using a second porosity factor as shown in [5]. Therefore, the AC resistance of the round conductor can be expressed similarly to equation (3)) as given in [5].

## 4 Core Losses

The core losses mainly depend on the material type, flux density and operating frequency. Although, there are many methods to estimate the core losses as reviewed in [18], the most common method is to use a power equation, which is known as the Steinmetz equation:

$$P_{core} = Kf^a B^b \quad (6)$$

where  $f$  is the operating frequency,  $B$  is peak magnetic flux density,  $K$ ,  $a$  and  $b$  are factors determined by the material characteristic obtained from the manufacturer's data.

Steinmetz equation is usually well established method for line transformers, in which sinusoidal excitation is used. However, in the medium-high

frequency transformers, the transformer is excited using power electronics (usually a square waveform, or stepped waveform), and transformer voltage and current include many harmonics.

#### 4.1 Core Losses in Non-Sinusoidal Excitation

Various methods are developed to model the core losses under non-sinusoidal excitation [19, 20]. Some of the methods reviewed in [5] can be listed as:

- Modified Steinmetz Equation
- Improved Generalized Steinmetz Equation
- Equivalent Elliptical Loop
- Waveform Coefficient Steinmetz Equation

In [19], a model has been developed to predict the non-sinusoidal excitation losses using just the standard Steinmetz parameters. The model calculates the total loss by adding the losses in major and minor loops in the voltage waveform.

Although these methods can provide more accurate results compared to Fourier transform method, they all require extra measurement steps to determine the material characteristics at different operating frequencies and waveforms. Therefore, it is impractical to use these models without experimental study at first. Therefore, using standard Steinmetz equation with harmonics contents is an ideal choice for analytical core loss estimation.

For non-sinusoidal waveforms, the easiest way to calculate the core losses is to use Fourier transform to get the frequency components and then to estimate individual core losses for each component.

The transformer developed by Narec will be excited using a square waveform in the low voltage side, and a multi-level inverter will be used in the high voltage side.

The core losses resulting from the low-voltage square wave excitation can be calculated by expressing the square wave as a Fourier series:

$$f(x) = \frac{4}{\pi} \sum_{n=1,3,5,\dots}^{+\infty} \frac{1}{n} \sin(n\omega x) \quad (7)$$

where  $\omega$  is the frequency of the square waveform in radians/s,  $n$  is the harmonic order. The magnitudes of the Fourier series components of the square wave relative to the magnitude of the square wave is presented in Table 5.

Harmonic Order	Magnitude
1	1.273
3	0.424
5	0.254
7	0.182
9	0.141
11	0.116
13	0.098

Table 5: Fourier series magnitudes relative to the magnitude of the square wave.

## 5 Modeling of the Transformer

A Matlab model is developed to estimate the transformer models and calculate copper and core losses. The design methodology used in the Matlab code is depicted in Fig. 10.

### 5.1 Estimation of Winding Parameters

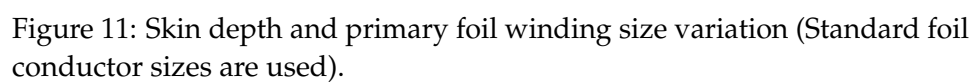
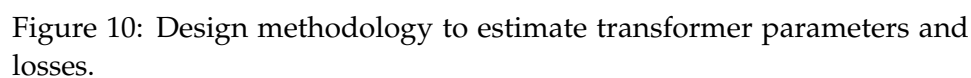
It is assumed from the WP 2 report that, foil type conductors are the most suitable option for the low voltage side. On the high voltage side, circular stranded cables are more suitable with their mechanical strength and increased dielectric insulation. It is stated in [13] that, using standard high-voltage cables has advantages such as: elimination of oil insulation, and better distribution of electric field in round conductors.

The thickness of the coil is chosen according to the skin depth at the operating frequency. The conductor thickness is selected to be less than 1.5 times skin depth, however, actual foil conductor thickness is limited to standard wire gauges (e.g. 1 mm, 1.6 mm, 2 mm, 2.25 mm...). The frequency of the transformer versus the most suitable foil coil thickness is plotted in Fig. 11. For example, for operating frequencies between 2 kHz and 3 kHz, the most suitable conductor thickness is 2 mm.

Then, using rated current and the rated current density, the required conductor area can be calculated. The conductor height can be found by dividing the conductor area to conductor thickness. For example, assuming a current density of  $4 A/mm^2$ , the foil conductor height can be calculated as a function of the operating frequency as shown in Fig. 12.

Similar method can be used for the secondary HV winding, where a standard circular HV cable can be used. The standard diameter of these cables are 2.5 mm, 4 mm, 6 mm, 10 mm, 16 mm. More information about





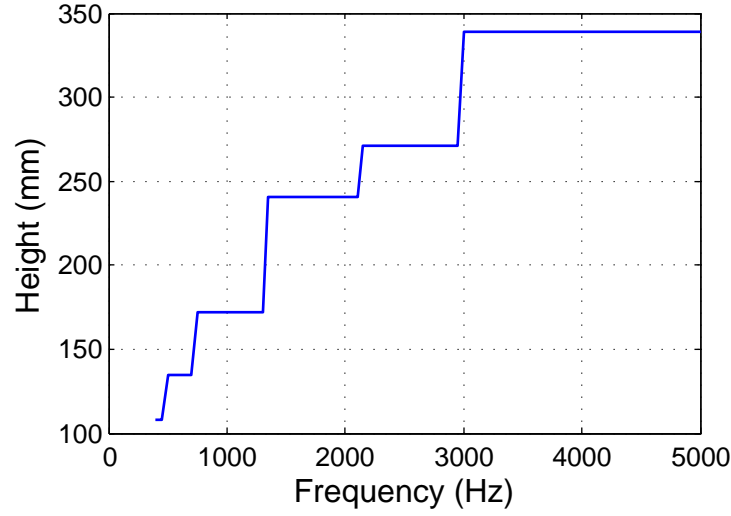


Figure 12: Height of the foil conductor as a function of the operating frequency.

Insulation Type	Material	Dielectric Strength
Potted	Epoxy	16 kV/mm
Potted	Micares	8-24 kV/mm
HV Cable	Silicone	4-28 kV/mm
HV Cable	PVC	10-10 kV/mm
HV Cable	HDPE	19 kV/mm

Table 6: Dry-type insulation dielectric strengths [7].

HV cables can be found in [21].

Insulation parameters should be known to determine the dimensions of the primary and secondary windings. Dry insulation is considered to be the most suitable insulation type due to increased reliability and ease of manufacturing. However, oil flooded windings can be preferred to improve thermal performance. In Table 6, dielectric strengths of some common dry-type insulation materials are presented and typical insulation thickness values are presented in [7]. Although, type of the insulation material is not specified in this report, but it is stated in WP2 report that the most suitable insulation type is potted epoxy. Following insulation thickness values are chosen to calculate AC copper losses. In order to get more accurate results, these values should be modified in the model once the detailed design of the transformer is completed.

- Insulation thickness between primary (low voltage) conductors: 1 mm
- Insulation thickness from primary winding to core: 10 mm
- Outer insulation thickness around primary winding: 10 mm
- Insulation thickness between secondary (high voltage) conductors: 5 mm
- Insulation thickness from secondary winding to core: 20 mm
- Outer insulation around secondary winding: 20 mm
- Insulation thickness between primary and secondary windings: 50 mm

## 5.2 Estimation of Core Dimensions

The most important parameter of the core is the cross-section area, which depends on the operating frequency, flux density in the core and the number of turns. Assuming a square cross-section area, the thickness of the core as a function of the primary number of turns is estimated as in Fig. 13, and similarly graphs for the secondary number of turns are presented in Fig. 14. The operating flux density of the core is assumed as 1.1 T, the primary voltage magnitude is assumed as 3 kV, and the secondary voltage magnitude is assumed as 300 kV.

Although, it is not presented in this report, the main dimensions and the mass of the core is calculated in the Matlab models and these figures can be used to estimate the overall weight and cost of the transformer.

## 6 Conclusion

In this report, a review of core materials and loss calculation methods for medium frequency transformers are presented. Following conclusions can be drawn from the report:

**Core Material:** Although electrical steel laminations are commonly used in line frequency transformers, they are not suitable in medium frequency transformers with their increased losses. Ferrites have very low losses, but they also have a very low operating flux density, which makes them unsuitable for high power applications. Nano-crystalline material is considered to be most suitable material with its high flux density and very low losses at high frequencies. Vacuumschmelze's Vitroperm500F is a popular material, that can be used. Amorphous materials can be used to reduce the core mass, as their operating flux densities are 25% higher than nano-crystalline materials, but they have higher losses.

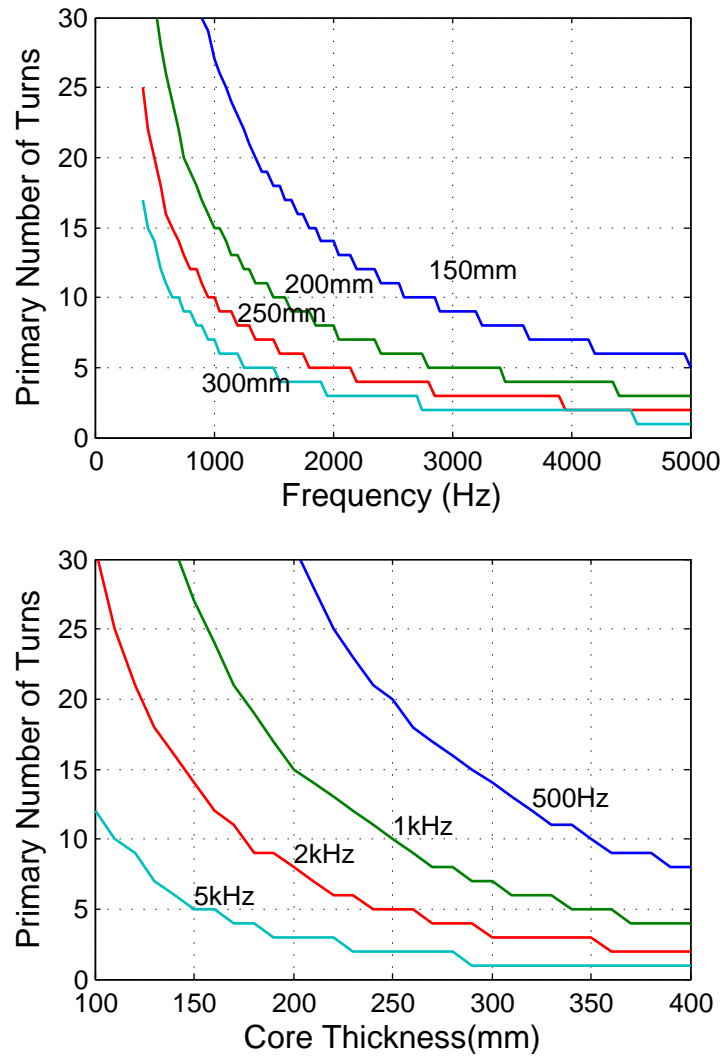


Figure 13: Core-thickness (assuming square cross-section area) as a function of the primary number of turns and operating frequency ( $B=1.1$  T,  $V_{in}=3$  kV,  $V_{out}=300$  kV).

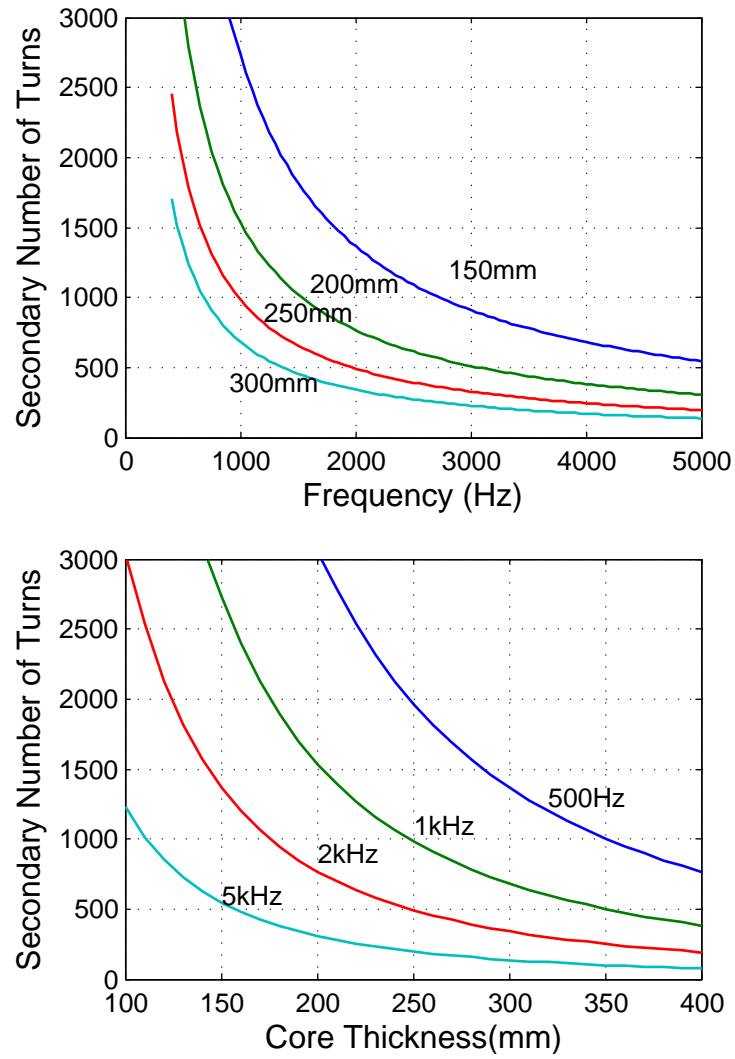


Figure 14: Core-thickness (assuming square cross-section area) as a function of the secondary number of turns and operating frequency ( $B=1.1$  T,  $V_{in}=3$  kV,  $V_{out}=300$  kV).

**Core Type:** Various transformer core topologies are compared in [1]. It is considered that core type transformer is the simplest and easiest to manufacture, and hence the most suitable option as the initial prototype.

**Winding Type:** In the primary field windings, the most suitable winding type is foil-type conductors, as low thickness is required for minimum eddy current loss, but a large conductor area is required to conduct high input current. It is possible to use two parallel primary windings to double the conducting area. Standard HV cables are proposed to be used in the secondary winding in order to simplify the manufacturing and insulation. Multi-stranded insulated conductors can be used to minimize the eddy current losses as a replacement to Litz wires.

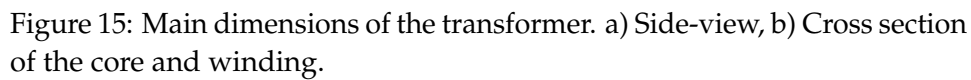
Matlab models are developed to estimate basic dimensions of the transformer core and winding. These parameters can be used as an input to finite element models or for a more detailed analytical models. In order to calculate the core losses accurately, the loss mapping of the material with magnetic flux and operating frequency should be known. This can be obtained from the manufacturer directly for some common materials, but a better option is to setup a small experimental rig to obtain these values.

## References

1. Edris Agheb and Hans K. Hoidalén. Medium frequency high power transformers, state of art and challenges. In *2012 International Conference on Renewable Energy Research and Applications (ICRERA)*, pages 1–6. IEEE, November 2012.
2. Michael Steiner and Harry Reinold. Medium frequency topology in railway applications. In *2007 European Conference on Power Electronics and Applications*, pages 1–10. IEEE, 2007.
3. Anish Prasai, Deepak Divan, Ashish Bendre, and Frank Kreikebaum. A new architecture for offshore wind farms. In *2007 European Conference on Power Electronics and Applications*, pages 1–10. IEEE, 2007.
4. Lothar Heinemann. An actively cooled high power, high frequency transformer with high insulation capability. In *APEC. Seventeenth Annual IEEE Applied Power Electronics Conference and Exposition (Cat. No.02CH37335)*, volume 00, pages 352–357. IEEE, 2002.
5. Irma Villar. *Multiphysical characterization of medium-frequency power electronic transformers*. Phd dissertation, École Polytechnique Federale de Lausanne, 2010.
6. G Ortiz, J Biela, D Bortis, and J. W. Kolar. 1 Megawatt, 20 kHz, isolated, bidirectional 12kV to 1.2kV DC-DC converter for renewable energy applications. In *The 2010 International Power Electronics Conference - ECCE ASIA -*, pages 3212–3219. IEEE, June 2010.
7. G. Ortiz, J. Biela, and J. W. Kolar. Optimized design of medium frequency transformers with high isolation requirements. In *IECON 2010 - 36th Annual Conference on IEEE Industrial Electronics Society*, pages 631–638. IEEE, November 2010.
8. Vacuumschmelze. Vitroperm 500 F - VitroVac 6030 F. Technical report.
9. MK Magnetics. Nanocrystalline: A Special Product Announcement.
10. Vacuumschmelze. Nanocrystalline VITROPERM. Technical report.
11. Vacuumschmelze. VITROPERM 500F Toroidal Cores. Technical report.
12. M Pavlovsky, S.W.H. de Haan, and J.A. Ferreira. Concept of 50 kW DC/DC converter based on ZVS, quasi-ZCS topology and integrated thermal and electromagnetic design. In *2005 European Conference on Power Electronics and Applications*, pages 9 pp.–P.9. IEEE, 2005.
13. J Morren, SWH de Haan, and JA Ferreira. High-voltage DC-DC converter for offshore windfarms. *IEEE Young Researchers Symposium in Electrical Power Engineering*, pages 1–6, 2002.

14. T Filchev, J Clare, P Wheeler, and R Richardson. Design of high voltage high frequency transformer for pulsed power applications. In *IET European Conference on European Pulsed Power 2009. Incorporating the CERN Klystron Modulator Workshop*, pages P18–P18. IET, 2009.
15. P.L. Dowell. Effects of eddy currents in transformer windings. *Proceedings of the Institution of Electrical Engineers*, 113(8):1387, 1966.
16. X Nan and C.R. Sullivan. An improved calculation of proximity-effect loss in high-frequency windings of round conductors. In *IEEE 34th Annual Conference on Power Electronics Specialist, 2003. PESC '03.*, volume 2, pages 853–860. IEEE, 2003.
17. J.a. Ferreira. Improved analytical modeling of conductive losses in magnetic components. *IEEE Transactions on Power Electronics*, 9(1):127–131, 1994.
18. Wei Shen. *Design of High-density Transformers for High-frequency High-power Converters*. PhD thesis, Virginia Polytechnic Institute and State University, 2006.
19. K. Venkatachalam, C.R. Sullivan, T Abdallah, and H Tacca. Accurate prediction of ferrite core loss with nonsinusoidal waveforms using only Steinmetz parameters. In *2002 IEEE Workshop on Computers in Power Electronics, 2002. Proceedings.*, number June, pages 36–41. IEEE, 2002.
20. J. Reinert, Ansgar Brockmeyer, and R.W.A.A. De Doncker. Calculation of losses in ferro- and ferrimagnetic materials based on the modified Steinmetz equation. *IEEE Transactions on Industry Applications*, 37(4):1055–1061, 2001.
21. HV Cable Catalogue.
22. Vacuumschmelze. Vitroperm 500 F - Vitrovac 6030F - Tape-Wound Cores in Power Transformers for Switched Mode Power Supplies. Technical report, 2003.





In this section, four transformer designs will be presented with different primary number of turns. The initial designs are developed the Matlab model described in the previous section.

- Operating Frequency: 1 kHz
- Core Material: Vitroperm 500F
- Operating Flux Density: 1.1 T (90% of the saturation flux density)
- Operating Temp: 110 C (for resistance calculations)
- Current Density: 4 A/mm<sup>2</sup> (in the conductor).
- Permeability:  $\mu = 30000$
- Core Type: C-core with square cross-section.
- LV Coil Type: Foil type conductor. The thickness is calculated considering eddy current loss as described in the previous section.
- HV Coil Type: Round insulated HV cable.
- Inner Insulation Thickness(Insulation between winding and the core):  
6 mm for the low-voltage side, 20 mm for the high-voltage side.
- Outer Insulation Thickness: 10 mm for the low-voltage side, 20 mm for the high-voltage side.
- Insulation Thickness Between Conductors: 1 mm for the primary coil, 5 mm for the secondary.
- Gap Between LV and HV Winding: 50 mm

	$N_{turns_{LV}}$	LV Winding	HV Winding	Core Mass
Design A	5	8.3 m	1159 m	2477 kg
Design B	8	11.0 m	1889 m	1500 kg
Design C	12	14.4 m	3146 m	1037 kg
Design D	15	17.0 m	4358 m	877 kg

Table 7: Variation of conductor length and core mass with number of turns.

Four Designs are presented in this report with varying primary(low-voltage) number of turns:

- Design A:  $N_{turns_{LV}} = 5$
- Design B:  $N_{turns_{LV}} = 8$
- Design C:  $N_{turns_{LV}} = 12$
- Design D:  $N_{turns_{LV}} = 15$

The specifications of these designs are presented through Table 8 to Table 11. Core mass, LV and HV conductor length variation are presented in Table 7. From the table, following can be concluded:

- Core mass reduces as the number of turns increases.
- The length of both windings increase with number of turns. However, increase in the LV winding length is less compared to HV winding length. For example, when primary number of turns is increased from 5 to 15, the length of the LV winding just doubles, however, the length of HV winding quadruples, which makes the losses in the HV side more dominant. This is due to thick insulation around the HV cable and high number of turns.
- Assuming the core loss is proportional to core mass and the copper loss is proportional to conductor length, the core loss reduces with increasing number of turns, whereas the copper loss increases with increasing number of turns.

The optimum number of turns is selected as 8 for the FEA simulations. FEA simulations are performed with Opera 3D software and the model building scripts can be found in the project folder.

Primary(LV)	Nturns=5
Coil Height	172 mm
Total Height	192 mm
Coil Thickness	3.15 mm
Winding Width	20.75
$R_{in}$	254 mm
$R_{out}$	285 mm
Mean Length	1662 mm
AC Resistance	0.0034 $\Omega$
Secondary (HV)	
Coil Area	6 mm <sup>2</sup>
Winding Height	152 mm
Total Height	192 mm
Ncoil horizontal	25
Ncoil vertical	20
Winding Width	202 mm
$R_{in}$	268 mm
$R_{out}$	490 mm
Mean Length	2319 mm
Core	
Thickness	351 mm
Cross Section	0.1228 m <sup>2</sup>
Horizontal Gap	474 mm
Vertical Gap	192 mm
Height	894 mm
Width	1176 mm
Volume	0.337 m <sup>3</sup>
Mass	2477 kg

Table 8: Design-A ( $N_{turns_{LV}} = 5$ ) winding and core parameters.

Primary (LV)	Nturns=8
Coil Height	172 mm
Total Height	192 mm
Coil Thickness	3.15 mm
Winding Width	33 mm
$R_{in}$	202 mm
$R_{out}$	245 mm
Mean Length	1377 mm
AC Resistance	0.011 $\Omega$
Secondary (HV)	
Coil Area	6 mm <sup>2</sup>
Winding Height	152 mm
Total Height	192 mm
Ncoil horizontal	40
Ncoil vertical	20
Winding Width	318 mm
$R_{in}$	216.5 mm
$R_{out}$	555 mm
Mean Length	2361 mm
Core	
Thickness	278 mm
Cross Section	0.0767 m <sup>2</sup>
Horizontal Gap	572 mm
Vertical Gap	192 mm
Height	748 mm
Width	1148 mm
Volume	0.204 m <sup>3</sup>
Mass	1500 kg

Table 9: Design-B ( $N_{turns_{LV}} = 8$ ) winding and core parameters.

Primary (LV)	Nturns=12
Coil Height	172 mm
Total Height	192 mm
Coil Thickness	3.15 mm
Winding Width	50 mm
$R_{in}$	166.5 mm
$R_{out}$	226 mm
Mean Length	1202 mm
AC Resistance	0.0323 $\Omega$
Secondary (HV)	
Coil Area	6 mm <sup>2</sup>
Winding Height	152 mm
Total Height	192 mm
Ncoil horizontal	60
Ncoil vertical	20
Winding Width	473 mm
$R_{in}$	180.5 mm
$R_{out}$	674 mm
Mean Length	2622 mm
Core	
Thickness	227 mm
Cross Section	0.0512 m <sup>2</sup>
Horizontal Gap	572 mm
Vertical Gap	192 mm
Height	646 mm
Width	1177 mm
Volume	0.141 m <sup>3</sup>
Mass	1037 kg

Table 10: Design-C ( $N_{turns_{LV}} = 12$ ) winding and core parameters.

Primary (LV)	Nturns=15
Coil Height	172 mm
Total Height	192 mm
Coil Thickness	3.15 mm
Winding Width	62.5 mm
$R_{in}$	149.5 mm
$R_{out}$	222 mm
Mean Length	1135 mm
AC Resistance	0.0593 $\Omega$
Secondary (HV)	
Coil Area	6 mm <sup>2</sup>
Winding Height	152 mm
Total Height	192 mm
Ncoil horizontal	75
Ncoil vertical	20
Winding Width	597 mm
$R_{in}$	163 mm
$R_{out}$	781 mm
Mean Length	2905 mm
Core	
Thickness	203 mm
Cross Section	0.0409 m <sup>2</sup>
Horizontal Gap	850 mm
Vertical Gap	192 mm
Height	598 mm
Width	1256 mm
Volume	0.119 m <sup>3</sup>
Mass	877 kg

Table 11: Design-D ( $N_{turns_{LV}} = 15$ ) winding and core parameters.

Frequency	Loss
1 kHz	0.25 W/kg
5 kHz	4.8 W/kg
10 kHz	17.5 W/kg
15 kHz	37.1 W/kg
20 kHz	63.3 W/kg

Table 12: Variation of core loss of Vitroperm 500 with frequency.

## 8 Core Losses

Core material is chosen as nano-crystalline (Vitroperm 500), the operating flux density is determined as 1.1 T. In the material manual [22], the core losses between 20 kHz and 100 kHz are presented. The loss data between 1 kHz and 10 kHz have been extrapolated using this data and data-sheets of similar materials. The core losses increase with the square of the magnitude of the flux density.

The core loss density variation with varying frequency is presented in Table 12.

The loss density (W/kg) data as a function of the flux density presented in the data-sheet are linear in log-x and log-y axes.

I have attached a spreadsheet presenting the losses between 1 kHz and 20 kHz for various operating flux densities, which can be used in the optimization algorithm. For information at 1 T loss density varies as follows: